Radiative Lifetimes of Some $3p$ and $3p'$ Levels of O II†

James H. Clark* and Charles E. Head
Department of Physics, Louisiana State University, New Orleans, Louisiana 70122
(Received 21 June 1971; revised manuscript received 31 March 1972)

The mean radiative lifetimes of several excited levels of O II have been measured using O_2^+ and O^+ ion beams in the 20–30-keV energy range. The levels were populated by directing the beams through a differentially pumped collision cell containing gaseous helium at pressures of a few mTorr. The decays in the intensities of selected electronic transitions, arising from the levels of interest, were obtained as a function of the distance x downstream from the exit aperture by using a $\frac{1}{2}$-m grating monochromator equipped with a photomultiplier detector. These decay curves were fitted to an expression of the form $I = A\, e^{-x/v\tau_k} + \sum_j B_j e^{-x/v\tau_j} + Ce^{-k'x}$, where A, B_j, and C are constants, v is the speed of the ions, τ_k is the lifetime of the level k of interest, τ_j is the lifetime of a level j which cascades into level k, and k' is a decay constant associated with the drop in gas pressure downstream from the exit aperture of the collision chamber arising from gas streaming through the aperture. The intensity data and the computed fits were plotted either by hand or by a plotter connected to a computer. The number of exponentials in a given fit was adjusted until a good fit was obtained, as determined by visual inspection in conjunction with a χ^2 test. Lifetimes (in nsec) obtained in this way are as follows: $\tau(3p\ ^4D^0_{7/2,1/2}) = 15.0 \pm 0.8$, $\tau(3p\ ^4D^0_{5/2}) = 14.9 \pm 0.4$, $\tau(3p\ ^4D^0_{3/2}) = 15.6 \pm 0.5$, $\tau(3p\ ^4P^0_{5/2,3/2}) = 8.5 \pm 0.6$, $\tau(3p\ ^2D^0) = 11.6 \pm 0.3$, $\tau(3p\ ^2P^0) = 9.2 \pm 0.1$, $\tau(3p'\ ^2F^0) = 12.1 \pm 0.3$, and $\tau(3p'\ ^2D^0) = 9.2 \pm 0.4$. These results are believed to be good to 10% or better. In addition to these results, measurements were also made on several other levels with lifetimes in the 6-nsec range. The reported values for the latter levels are upper limits to the actual lifetimes and are otherwise unreliable because of the possibility of significant errors arising from gas streaming. An extensive discussion of the treatment of possible errors from gas streaming, cascading, and blending of spectral lines is given.

I. INTRODUCTION

In this paper we report the results of an investigation, using the ion-beam method with a gas target, of the mean radiative lifetimes of several excited electronic energy levels of O^+(O II). In view of many improvements in apparatus and techniques since the first detailed paper[1] from this laboratory, we begin by reviewing the pertinent details of our apparatus and the methods used in acquiring and reducing the data. The principal sources of errors are discussed and their effects are noted.

Results are presented for the $3p\ ^4D^0$, $3p\ ^4P^0$, $3p\ ^2D^0$, $3p\ ^2P^0$, $3p'\ ^2F^0$, and $3p'\ ^2D^0$ levels of O II. Measurements for these levels are believed to be reliable to better than 10%. In addition, apparent lifetimes are presented for the $3p\ ^4S^0$, $3d\ ^4F$, $3p'\ ^2P^0$, $3d'\ ^2G$, and $4f'\ ^2H^0$ levels. Our reported lifetimes for these levels should be taken as upper limits on the true lifetimes of the respective levels.

II. APPARATUS AND EXPERIMENTAL PROCEDURE

A description of the positive-ion accelerator used in our work is given in Ref. 1. Since that paper appeared we have completely rebuilt the accelerator; but the basic details of its construction remain approximately the same. Major modifications, however, have been made in the collision chamber and observation chamber.

A magnetically analyzed beam of ions was passed through a gas-filled collision chamber 5 cm long into a differentially pumped observation chamber via two 0.096-in.-diam holes. Inside the collision chamber the excited levels of the ions were populated by collisions with the target-gas atoms. These levels then decayed as the fast beam ions passed into and across the observation chamber. Light from the radiative decay of the levels was focused, under unit magnification, onto the entrance slit of a Jarrell-Ash 0.5-m scanning monochromator for analysis. The decay of the intensity of a particular transition was then recorded as the monochromator was translated downstream from the exit aperture of the collision chamber.

The window in the observation chamber and the lens (focal length of 12 cm) were made of fused quartz to aid investigations in the near ultraviolet.

The ion beam was imaged across the entrance slit of the monochromator with the axis of the beam image perpendicular to the slits. Since both the entrance slit and the exit slit were 2 cm high and since the beam was only approximately 2.5 cm in diameter, no light was likely to be lost as the monochromator was moved downstream parallel to the beam axis. Nevertheless, care was always taken to ensure that the beam remained centered in the slits at the extremes of its travel.

The monochromator was equipped with an EMI 6256QB end-on photomultiplier (PM) tube. For especially weak signals an EMI 6256QS tube was

used in order to reduce the dark current (count). The PM detector was housed in a μ-metal shield to eliminate the effects of stray magnetic fields.

During the course of our investigation of the O II lifetimes, we used three different methods of processing the signals from the PM tube. Originally, the anode current from the tube was fed into a Jarrell-Ash electrometer amplifier; and the amplified signal was recorded on a strip-chart recorder. Later, a pulse amplifier and single-channel analyzer were substituted for the electrometer amplifier; and the signal was stored in a Nuclear Data series 2200 multichannel analyzer (MCA). In the third arrangment the signal was fed into a scaler controlled by an electronic timer. The timer also controlled a second scaler into which was fed the shaped and amplified signal of a second photomultiplier which measured the intensity of a particular transition at a fixed region in the ion beam.

In the first method the beam current was collected in a deep cup, was fed into a Keithley model 414 or model 410 micromicroammeter, and was recorded on a Keithley model 370 chart recorder. With the monochromator at a fixed position, both the transition intensity and the beam current were recorded simultaneously for 1–5 min, depending on the strength of the transition. A background reading was then taken for both signals. The signals were then further visually averaged using a ruler and pen. The monochromator was then moved to a different position and the whole procedure was repeated. Data runs taken in this fashion usually consumed 2–5 h per run.

In the second method used, the shaped and amplified pulses from the PM tube were fed into the MCA while the monochromator was being translated downstream from the collision cell at a uniform rate. The MCA was used in a multiscale mode with dwell times of 0.8 sec per channel. With 512 channels, a run was completed in approximately 6.8 min instead of 2–5 h. The principal difficulty with this method was that it was necessary to keep the beam current constant for the entire duration of the run. A run was rejected if the area bounded by the actual current trace and the average current signal (drawn with pen and ruler) exceeded approximately 1% of the area under the average signal. For the majority of the data taken with the MCA, however, no difficulty with current fluctuation was encountered. For the most part, we did not start a data run unless the current trace was a straight line on the strip-chart recorder. In practice, this meant that it was necessary to recondition the rf ion source much too often, usually every few days.

These difficulties with methods 1 and 2 led us to consider the present setup. We now record the beam-current signal by measuring the intensity of a strong transition from the beam (in this case an O II transition) in a fixed region near the exit aperture of the collision chamber with a second PM tube. This tube is mounted over the exit slit of a 0.25-m Jarrell-Ash manually operated monochromator. The pulses from this PM tube are shaped and amplified by an ORTEC model 486 amplifier-pulse height analyzer and counted by an ORTEC model 431A timer scaler. The signal from the PM tube measuring the intensity at different points along the beam is fed into an identical combination of ORTEC electronic equipment. The scalers recording both signals are controlled by the same ORTEC model 431B timer scaler used in the timer mode.

Results using all three methods are in agreement within the usual statistical uncertainties.

The critical parameter for our apparatus is the transition decay length $v\tau$, where v is the speed of the ions and τ is the lifetime of the upper level of the transition. Slit widths on the main monochromator must be chosen such that they are less than $v\tau$, but not so small that the signals become too weak. At the same time, care must be taken to ensure that no blending with spectral lines of unwanted transitions is taking place. Our monochromator has a reciprocal linear dispersion of 16 Å/mm; thus, the maximum slit width w, in mm, which can be used is given by $w = \frac{1}{16}\Delta\lambda$, where $\Delta\lambda$ is the maximum spectral window, in Å, which permits the transition of interest to be resolved from unwanted transitions. In practice, this width is usually very small compared to $v\tau$, typically being in the range from 0.1 to 0.4 mm. The measured decay lengths are greater than 2.5 mm.

The target gas used to excite the O II transitions was helium. Pressures used in the collision chamber ranged from a few mTorr up to 70 mTorr for a few decay curves. A Pirani gauge calibrated with a McLeod gauge was used to monitor the pressures in the collision cell. Readings were checked frequently to assure constancy of gas pressure; and, as a double check, numerous overlap data points were frequently taken. No dependence of the measured lifetimes on the target-gas pressure was observed.

Streaming of the target gas through the beam exit aperture in the collision chamber might have introduced major systematic errors into our data. Consequently, we made extensive studies to determine not only the pressure differential between the interior of the collision chamber and a fixed point at the downstream end of the observation chamber, but also the variation of the gas pressure across the observation region. The pressure at the downstream end of the observation region was measured using a hot-cathode ionization gauge.

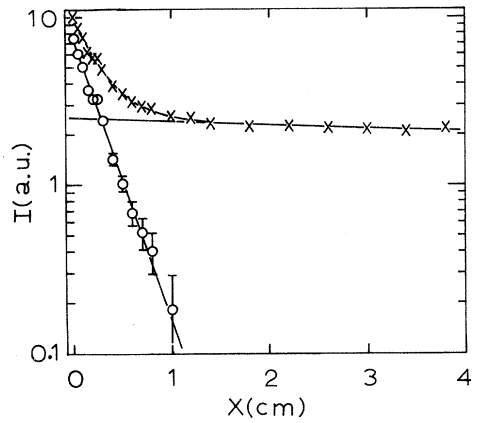

FIG. 1. Decay of the intensity I, in arbitrary units (a.u.), of the target He λ(5875.7-Å) line as a function of the distance x downstream from the exit aperture of the collision chamber. The experimental points (×) have been fitted with the sum of two exponentials (straight lines). The open circles (○) represent the experimental points after the slowly decaying exponential has been subtracted. The decay constants from a computerized least-squares fit were 3.89 and 0.0465 cm^{-1}, respectively, for the fast component and the slow component. The χ^2 integral for the fit is 0.914. The O_2^+ beam energy was 24.4 keV.

Typical pressures at this point ranged from 1×10^{-5} to 5×10^{-5} Torr. The corresponding target-gas pressure in the collision chamber ranged from 10 to 50 mTorr, respectively. (That is, for a pressure of 30 mTorr in the collision chamber, the indicated pressure in the observation chamber was approximately 3×10^{-5} Torr.) Clearly, the indicated pressure differential was 1000 to 1; but, allowing for the possibility of gauge calibration errors, we claim only an indicated pressure differential greater than or equal to 200 to 1 for the downstream side of the observation region.

The pressure in the observation region with no target gas was less than 10^{-6} Torr.

The pressure across the observation region was measured by monitoring the variation in intensity of two target He I emission lines with distance downstream from the exit aperture of the collision cell. Typical curves of the λ(5876-Å) and λ(3889-Å) lines of He are shown in Figs. 1 and 2. They are tracings of graphs generated and plotted by a computer. These curves were taken with an O_2^+ beam at 3×10^{-2}-Torr helium target pressure and 3×10^{-5} Torr indicated observation-chamber pressure (downstream end). The energy of the beam was 24.4 keV and the beam current was approximately 0.8 μA. The monochromator slit width used for Fig. 1 was 0.4 mm; and for Fig. 2, 0.25 mm.

The first point of each curve has been normalized to 10 by the computer program used in fitting the data. [The actual numbers of counts for the first point of the λ(5876-Å) curve are 7658 counts for the intensity detector which is translated and 148 114 counts for the stationary detector.] The curve shown is the variation of intensity counts divided by current-detector counts (stationary PM tube) along the beam. Both signals were corrected for background light and dark counts before the division was effected. Because of the weak signal, the intensity-measuring PM tube was cooled, using dry ice, in order to reduce the dark count to around 5 counts/sec. (Data were usually accumulated in 10-sec intervals.) The counting rate for the PM tube used for the current detector was sufficiently high that cooling it was unnecessary. (The actual numbers of counts for the first point of Fig. 2 were 14 501 for the intensity detector and 169 288 for the current detector.)

Each of the curves in Figs. 1 and 2 has been fitted with the sum of two exponentials. The χ^2 integral is 0.91 for the former 1.00 for the latter. Unfortunately, our χ^2 test was not always reliable; and we had to make our final judgement on the quality of a fit by visual inspection. The indicated error bars were derived by assuming that the standard deviation of N counts was $N^{1/2}$. Error bars are not shown when the size of the point symbol exceeds the size of the error bars.

The χ^2 test was sometimes unreliable because of a constant random noise produced by our rf ion source. It did not appreciably affect our results, since it was subtracted out, but it tended to make our χ^2 integral values high. The problem has since been partially solved by better shielding and better

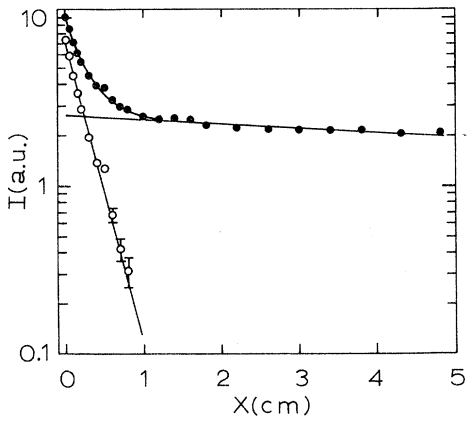

FIG. 2. Decay of the intensity I, in arbitrary units, of the target He λ(3888.65-Å) line as a function of the distance x downstream from the exit aperture of the collision chamber. The experimental points have been fitted with the sum of two exponentials with decay constarts of 4.15 and 0.0598 cm^{-1}. The χ^2 integral for this fit is 1.000, although the fit appears to be good. See text for discussion. The O_2^+ beam energy was 24.4 keV.

electronic discrimination. Recent results with good χ^2 integrals are in excellent agreement with earlier results.

The fits to the curves in Figs. 1 and 2 tell us that the number density of He atoms in the observation chamber drops approximately as the sum of a quickly decaying exponential (decay length 2.5 mm) and a slowly decaying one (decay length 19 cm). These results are in excellent agreement with an earlier study[2] in which a Ne^+ beam was used.

It is easy to associate the fast-decay component with the rapid $1/r^2$ drop in density associated with a point source of outgoing particles. Since the streaming He atoms in our apparatus soon encounter the walls of the observation chamber (2-in.-diam tubing) this initial rapid drop in number density is replaced by a less rapid drop associated with the diffusion of the gas across the observation region to the diffusion pump.

Extrapolation of the decay curves in Figs. 1 and 2 to the position of the ionization gauge yields the fact that the pressure of the gas in the observation region drops by a factor of 10 from the upstream end to the downstream end, again in agreement with the Ne study.[2] One may thus conclude that the pressure at the beginning of our decay curves is less than or equal to $\frac{1}{20}$ times that in the interior of the collision chamber. The presence of this gas in the observation region leads to some repopulation of the O^+ levels.

Oxygen was used as the source gas in our rf ion bottle. Beams of O_2^+ and O^+ were produced with analyzed collimated beam currents of approximately 1 and 0.1 μA, respectively. The weak O^+ beam currents led us to use the O_2^+ beam almost exclusively, with the exception of a few data runs to check consistency of results from the two beams.

III. DATA, ANALYSIS, AND RESULTS

The rate equations governing the decay of the intensity downstream from the collision cell have been treated extensively in Ref. 2; therefore, we shall review here only the essential features of the analysis.

If there were a sharp cutoff in the target gas at the exit collimator, then the rate equation for the number density N_k of atoms in excited state k would be given by

$$\frac{dN_k}{dx} = \frac{-N_k}{v\tau_k} + \frac{1}{v}\sum_j N_j A_{jk} , \tag{1}$$

where x is the distance downstream, τ_k is the mean lifetime of state k, v is the speed of the ions, N_j is the number density of atoms in excited state j ($E_j > E_k$; E being the energy), and A_{jk} is the transition probability per unit time for radiative transfer from j to k (cascading). If the cascade term were not present in Eq. (1), then N_k would be given by

$$N_k = N_{k0}\, e^{-x/v\tau_k} . \tag{2}$$

Since cascading is usually present in amounts varying from 3 to 40%, Eq. (1) can be solved approximately by assuming that the number density N_j of the levels j from which the cascade originates is given by an expression such as that in Eq. (2). This leads to a solution such as

$$N_k = Ae^{-x/v\tau_k} + \sum_{j>k} B_j e^{-x/v\tau_j} , \tag{3}$$

where A and B_j are constants.

Unfortunately, gas does stream through the exit aperture and does repopulate the excited states. With the appropriate correction, Eq. (1) becomes

$$\frac{dN_k}{dx} = \frac{-N_k}{v\tau_k} + \frac{1}{v}\sum_{j>k} N_j A_{jk} + \frac{\sigma_k \rho F}{v} , \tag{4}$$

where σ_k is the collision cross section for populating state k, ρ is the number density of the target gas, and F is the incident-beam particle flux. In order to solve this equation, one must know how ρ and F vary with x. For low target-gas pressures, F is approximately a constant over the region of observation and presents no real problem. The target density ρ, however, appears to vary approximately as the sum of two exponentials, as shown in Figs. 1 and 2. If we thus take ρ as

$$\rho = Ce^{-k_1 x} + De^{-k_2 x} , \tag{5}$$

k_1, k_2, C, and D being constants, we can easily solve Eq. (4) to obtain

$$N_k = A' e^{-x/v\tau_k} + \sum_j B' e^{-x/v\tau_j} + C' e^{-k_1 x} + D' e^{-k_2 x} . \tag{6}$$

Here, A', B'_j, C', and D' are constants, independent of x, but dependent on the τ's, k's, and v.

It should be noted here that we can sometimes fit the target He λ(5876-Å) and λ(3889-Å) curves with sums of two exponentials and a constant or with sums of three exponentials, the most quickly decaying component having a decay constant k of the order of 10 cm^{-1}. We believe that the intermediate component in these curves may arise from the He atoms gaining small velocity components downstream during the collisions with the beam ions and that the fastest decaying component is associated with the initial drop in target-gas pressure. More evidence to support this interpretation is presented later.

However, assuming a two-exponential decay in the target pressure in the observation region and using computer fits to Figs. 1 and 2, we obtain $k_1 \simeq 4.0$ cm^{-1} and $k_2 \simeq 0.053$ cm^{-1}. These values correspond to decay lengths of approximately 2.5 mm and 19 cm, respectively, as pointed out in Sec. II.

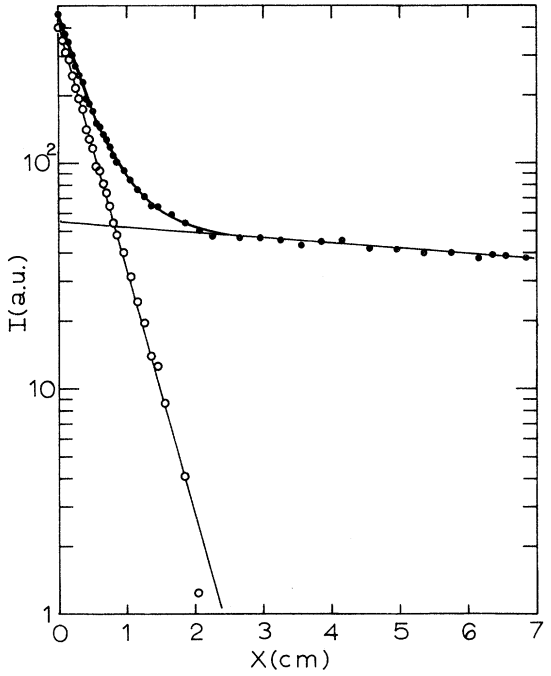

FIG. 3. Decay of the intensity I, in arbitrary units, of the combined O II λ(4414.91-Å) and λ(4416.98-Å) lines, orginating from $3p\,^2D^0$ levels, as a function of the distance x downstream from the exit aperture of the collision chamber. The energy of the O_2^+ beam ions used was 21.2 keV; the monochromator slit width used was 0.4 mm, corresponding to a spectral window of 6.4 Å. The beam current was approximately 0.5 μA. The experimental points were fitted with the sum of two exponentials, yielding 11.24 nsec for the lifetime of the $3p\,^2D^0$ levels. The decay length of the slowly decaying exponential obtained was 17.3 cm, in good agreement with the results from the target He lines.

Since the intensity of a transition originating from state k is proportional to N_k, we can extract τ_k by fitting an expression of the form of Eq. (6) to the observed decay curves. Theoretically, the minimum number of exponentials used in the fit should be three, if no cascading is present. We have found, however, that as long as $v\tau_k$ does not get too near k_1 in value, a fit with two exponentials suffices in some cases. This is possible because we first begin viewing the radiation several decay lengths downstream from the interior of the collision cell. At this point the $C_1' e^{-k_1 x}$ component has effectively died out. Thus, the only terms remaining in the fit are those corresponding to the first and last terms on the right-hand side of Eq. (6) in the absence of cascading. An example of this is illustrated in Fig. 3.

Theoretically, since C' is negative when $k_1 > (v\tau_k)^{-1}$, the third term in Eq. (6) contributes an initial buildup to the decay curve of the type shown in Fig. 4. Unfortunately, this effect is also present in the event of cascading from a short-lived state, thus making it difficult to identify with certainty the source of such contributions. In any case, these contributions can be eliminated by dropping the first few points in the decay curve from the fit, or, when the S/N ratio is sufficient, as in Fig. 4, by adding an extra exponential to the fit.

In the particular case cited above, cascading originating from the $2p^2(^3P)3d\,^4F$ levels may be present; for example, see Fig. 5. These levels have a theoretical lifetime[3] of 5.1 nsec, a value consistent with the lifetime of 5.13 nsec from the fit to the curve in Fig. 4. The latter value is also in agreement with our experimental measurement of 5.8 ± 0.5 nsec for the $3d\,^4F$ levels, obtained by using the $3d\,^4F \rightarrow 3p\,^4D^0$ transitions.

One may, however, reason that what we are seeing in both the $3d\,^4F$ and $3p\,^4D^0$ multiplets arises from the gas streaming through the exit aperture of the collision cell. If this were indeed the case, then the decay constants associated with the fast decays in these curves would be the same as the decay constants in the He decay curves. Further-

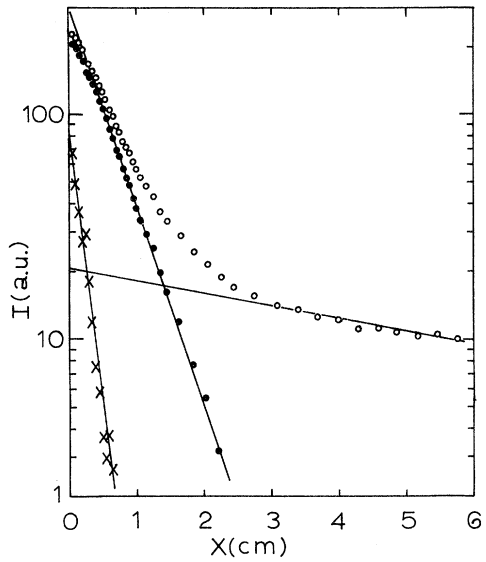

FIG. 4. Typical decay of the intensity I of the combined λ(4649.14-Å) ($J = \frac{7}{2}$) and λ(4650.84-Å) ($J = \frac{5}{2}$) lines of O II, originating from the $3p\,^4D^0$ levels. This curve was fitted with the sum of three exponentials. The indicated lifetimes of the components were 5.13, 13.70, and 222 nsec. The shortest-lived component (×) has a negative coefficient and could possibly arise from repopulation of the $3p\,^4D^0$ levels by the target gas streaming through the exit aperture; however, the most likely origin of this component is cascading from the $3d\,^4F$ levels. Pertinent experimental parameters were as follows: O_2^+ beam energy is 21.5 keV, beam current is $\simeq 1.25$ μA, and monochromator slit widths are 0.2 mm (spectral window is 3.2 Å).

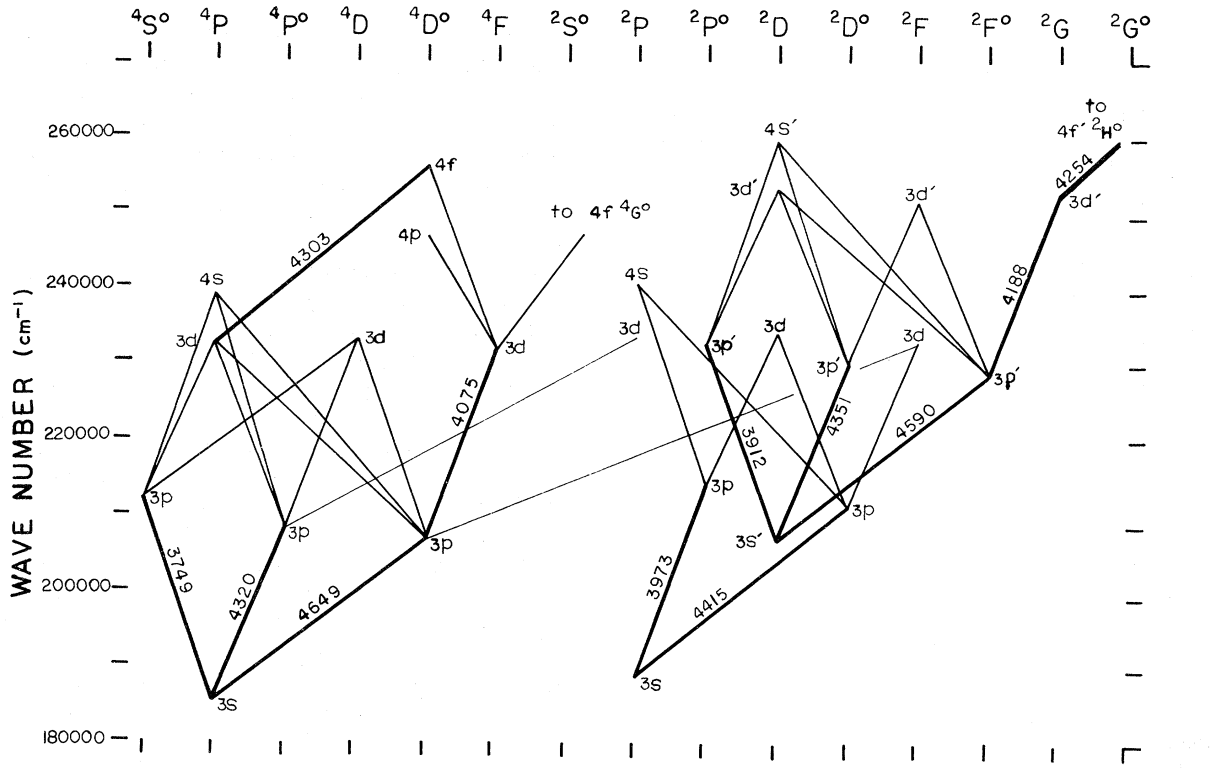

FIG. 5. Partial Grotrian diagram for O II. Indicated wavelengths are the approximate wavelength settings used on our monochromator to obtain the decay curves for the indicated transitions. See text for detailed descriptions of the various transitions.

more, these decay constants would not change in switching from an O_2^+ beam to an O^+ beam. This, therefore, would mean that the indicated lifetimes for the O^+ beam would be shorter by a factor of $\sqrt{2}$ than those for the O_2^+, if we were indeed riding down the pressure curve just outside the exit aperture. The factor of $\sqrt{2}$ follows from the fact that, for constant energy, the O_2^+ beam is $\sqrt{2}$ times slower than the O^+ beam. This result gave us the best check on the presence of systematic errors arising from streaming effects. (See the discussion of the results below.)

An example of a decay curve with an intermediate-lived decay component definitely arising from cascading is shown in Fig. 6.

A. $3p\,^4D^0 \rightarrow 3s\,^4P$

This multiplet gave rise to the most intense lines which we observed in the O_2^+ and O^+ beam spectra. These lines are shown in Fig. 7. The wavelength identifications given there have been made using scans taken with our monochromator, accurate to ± 1 Å, in conjunction with the National Bureau of Standards (NBS) tables by Wiese, Smith, and Glennon[3] and the recent English translation of the Russian wavelength tables by Zaidel' *et al.*[4] It is interesting to compare the experimentally obtained relative intensities of the individual spectral lines in Fig. 7 with the theoretical line strengths tabulated for O II in Ref. 3. These results are shown in Table I. The experimental values are accurate to only around ± 20% for the stronger lines because of occasional sharp drops in the O_2^+ beam current. With the exception of the λ(4673.75-Å) line, the agreement between theory and experiment is remarkably good.

The experimental values in Table I were reproducible from scan to scan within the experimental uncertainties. Within a given multiplet the relative experimental line intensities were found to follow, within the experimental error, the relative theoretical line strengths for all the transitions studied by us. This enabled us to estimate the extent of overlap with unwanted spectral lines, even in those cases where our monochromator did not have sufficient resolution to separate close-lying lines.

From the combined $3p\,^4D^0_{7/2} \rightarrow 3s\,^4P_{5/2}$ (λ = 4649.14 Å) and $3p\,^4D^0_{1/2} \rightarrow 3s\,^4P_{1/2}$ (λ = 4650.84 Å) transitions we obtained a value of 15.0 ± 0.8 nsec for the mean radiative lifetime of the combined $J = \frac{7}{2}$ and $J = \frac{1}{2}$ levels of the $3p\,^4D^0$ term. This value is the mean of the results from eleven independent decay curves. The uncertainty given is the standard

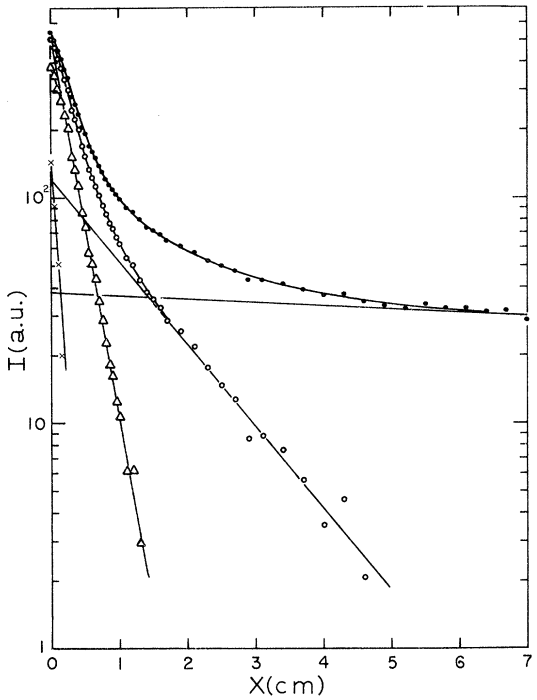

FIG. 6. Decay of the intensity I of the λ(4075.87-Å) line of O II with distance x downstream from the collision cell. The experimental data are represented by the solid dots (●). This curve was fitted with the sum of four exponentials, represented by the straight lines. The one with the largest slope has a negative coefficient (the absolute value is plotted) and is believed to originate from gas-streaming effects. The component with the smallest slope is also primarily due to gas streaming; however, the component with the next smallest slope (○) arises from cascading into the $3d\,^4F$ levels. The component fitted to the triangle (△) curve is identified with the natural decay of the $3d\,^4F$ levels. Beam data: 23.7 keV, 0.68 μA of O_2^+.

deviation of the measurements and gives an indication of the reproducibility of the results using different energies, different target-gas pressures, and different beam currents. It also gives an indication of the reliability of the curve-fitting procedure, since some runs were fitted with sums of three exponentials, when data near the exit aperture were used, and with sums of two exponentials, when the first few points were deleted.

The λ(4641.81-Å) line was used to obtain the lifetime of the $J=\frac{5}{2}$ levels. The average from seven different decay curves was 14.9 ± 0.4 nsec. One of the curves, shown in Fig. 8, was obtained using an O^+ beam; the others were taken with an O_2^+ beam. The fit to the O^+ data in Fig. 8 gave a value of 14.8 nsec, clearly in excellent agreement with the mean of all the runs. This can be interpreted as firm evidence that there are no systematic errors arising from gas streaming in these

TABLE I. Relative line strengths for the $3p\,^4D^0 \rightarrow 3s\,^4P$ multiplet in arbitrary units (a.u.).

λ (Å)[a]	Theoretical[a] (a.u.)	Experimental[b] (a.u.)
4638.85	8.3	10.2
4641.81	23.3	23.2
4649.14	41.1	41.1
4650.84	8.1	9.0
4661.64	10.4	10.7
4673.75	1.32	2.32
4676.23	7.8	7.4

[a]Taken from Ref. 3.

[b]Taken from Fig. 7. The experimental values are normalized using the theoretical value for the λ(4649.14-Å) line. They are accurate to approximately ± 20% for the stronger lines. Because of this large error, no wavelength corrections for the experimental line strengths have been applied in this or succeeding tables.

results. It should also be noted that the negative component of the curve in Fig. 8 gives a value of 5.3 nsec, in excellent agreement with the theoretical lifetime of 5.1 nsec for the $3d\,^4F$ levels which cascade into the $3p\,^4D^0$ levels (see Fig. 5).

The lifetime of the $J=\frac{3}{2}$ levels was obtained by measurements on the λ(4661.64-Å) line. The mean of three separate decay curves yielded a value of 15.6 ± 0.5 nsec.

All the above results are summarized in Table II, along with the results of other investigators[5,6] for comparison. Also given are the theoretical lifetimes calculated from Ref. 3 by taking the inverse of the sum of all transition rates out of the appropriate J levels.

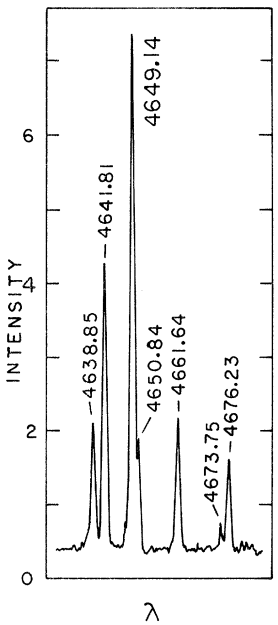

FIG. 7. Partial spectrum of an O_2^+ beam containing all but one of the components of the $3p\,^4D^0 \rightarrow 3s\,^4P$ multiplet of O II. The monochromator was positioned to view the beam at approximately 1 mm from the exit aperture of the collision cell. Wavelengths of the lines are shown in Å, and the intensity is given in arbitrary units.

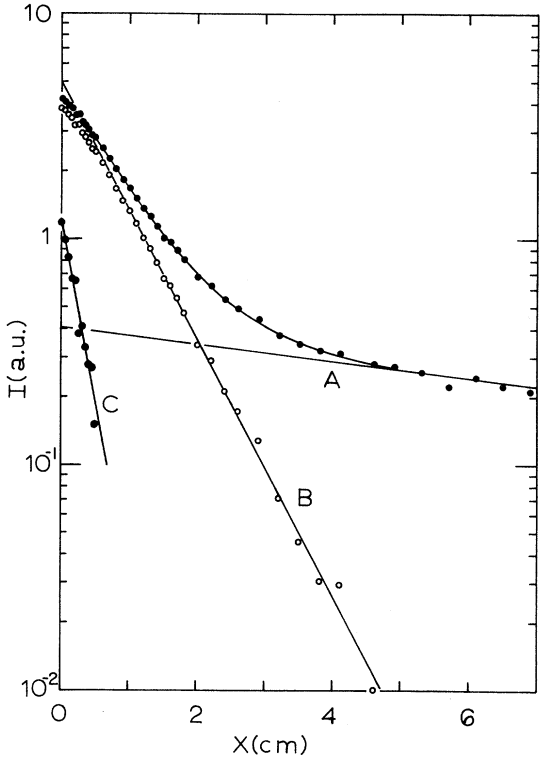

FIG. 8. Decay of the intensity I of the λ(4641.81-Å) line of O II with distance x downstream from the collision cell. An O^+ beam (22.1 keV, 0.2 μA) was used to obtain these data. The indicated lifetimes from the computerized fit to the sum of three exponentials were (A) 229 nsec, (B) 14.8 nsec, and (C) 5.26 nsec. The coefficient of the fast component (C) is negative, as in Fig. 4.

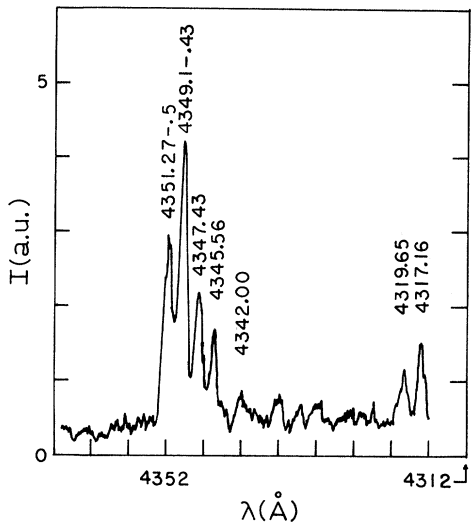

FIG. 9. Partial spectrum of an O_2^+ beam between approximately 4317 and 4362 Å containing the principal members of the $3p\ ^4P^0 \rightarrow 3s\ ^4P$ and the $3p'\ ^2D^0 \rightarrow 3s'\ ^2D$ multiplets of O II.

It is not likely that the lifetimes are very much dependent on the J value of the levels, as our results indicate; therefore, the scatter in Copeland's measurements[5] should be a measure of the reproducibility of his results. If this is indeed the case, then his values and ours are in agreement within the experimental error of both (see Sec. IV). The same thing might also be said of the work by Druetta, Poulizac, and Dufay[6]; however, it ap-

TABLE II. Lifetimes for the $2p^2(^3P)3p\ ^4D^0$ multiplet of O II.

Investigators	λ (Å)	τ (nsec) $J=\frac{7}{2}$	$J=\frac{5}{2}$	$J=\frac{3}{2}$	$J=\frac{1}{2}$
Clark and Head	4661.64, 4650.84, 4649.14	15.0 ± 0.8		15.6 ± 0.5	15.0 ± 0.8
	4641.81		14.9 ± 0.4		
Copeland[a]	4676.23		14.7		
	4673.75				14.4
	4661.64			13.0	
	4650.84				12.1
	4649.14	12.1			
	4641.81		11.6		
	4638.85			12.5	
Druetta, Poulizac, and Dufay[b]	4661.64			19	
	4649.14	10			
	4641.81		12		
Theory[c]		9.6	9.5	10.2	10.5

[a]Reference 5.
[b]Reference 6.
[c]Reference 3. In the LS coupling approximation, these values should all be the same.

TABLE III. Multiplets and relative line strengths in the range 4315–4360 Å in arbitrary units (a.u.).

Multiplet	λ(Å)	Theoret. line strength[a] (a.u.)		Obs. line strength[b](a.u.)
$3p\,^4p^0 \rightarrow 3s\,^4P$	4317.14	6.7		6.1
	4319.63	6.8		4.3
	4325.77	1.24		0.9
	4336.87	2.64		2.0
	4345.56	7.2		7.2[c]
	4349.43	18.1		N.R.[d]
$3p\,^4S^0 \rightarrow 3s\,^2P$	4329.0	0.0252		N.O.[e]
$3p'\,^2D^0 \rightarrow 3s'\,^2D$	4347.43	15.3		15.3[c]
	4349.1	1.65		N.R.[d]
	4351.27	23.6	25.4	22
	4351.5	1.82		
$3d'\,^2S \rightarrow 3p'\,^2P^0$	4319.93	4.83		very weak
	4328.62	9.7		or missing
$3d\,^2D \rightarrow 3p\,^2D^0$	4359.38			N.O.[e]
$4f\,^2G^0 \rightarrow 3d\,^2F$	4340.36	72		very
	4342.00	93		weak

[a]Taken from Ref. 3.

[b]Experimental line strengths are taken from Fig. 9. They are very approximate because of the poor S/N ratio and are intended only for use in checking for possible blending of lines.

[c]Line strengths within each multiplet were normalized using these lines.

[d]Not resolved from nearby line.

[e]Not observed.

pears that they may have made an erroneous identification of a decay component in their curves. Their paper indicates that a 12-nsec decay component was present in their λ(4661.64-Å) (4660-Å according to them) measurement which contributed one-third of the intensity initially. It is thus rather probable that their primary component in this line arose from unresolved blending or from cascading from a longer-lived level. If our interpretation is correct, then their results become self-consistent, but somewhat shorter than ours.

The method of measurement used by Copeland was pulsed-electron-beam excitation with delayed-coincidence detection. The method used by Druetta *et al.* was the beam-foil method.

B. $3p\,^4P^0 \rightarrow 3s\,^4P$

Figure 9 shows the portion of the observed spectrum of the O_2^+ beam between approximately 4317 and 4362 Å containing most of the members of this multiplet. It was taken with a spectral window of 1.12 Å in order to check for the existence of the $3d'\,^2S \rightarrow 3p'\,^2P^0$ and the $3p'\,^2D^0 \rightarrow 3s'\,^2D$ multiplets, in particular, since they could have presented blending problems for data taken with wide monochromator slit widths. The approximate line strengths of the lines observed have been tabulated in Table III, along with the theoretical line strengths from Ref. 3.

Since the λ(4328.62-Å) line is the strongest of the $3d'\,^2S \rightarrow 3p'\,^2P^0$ multiplet and since it was very weak or absent in all of the scans which we made over the region covered by Table III, we concluded that the weaker λ(4319.93-Å) line would not contribute significantly to decay curves taken on the combined λ(4317.14-Å) and λ(4319.63-Å) lines from the $3p\,^4P^0 \rightarrow 3s\,^4P$ multiplet. This enabled us to open the monochromator slits wide enough to obtain an acceptable S/N ratio. By contrast, the $3p'\,^2D^0 \rightarrow 3s'\,^2D$ multiplet can be seen in Fig. 9 to be quite intense and intermingled with the other lines of the $3p\,^4P^0 \rightarrow 3s\,^4P$ multiplet.

Using eight different decay curves taken on the combined λ(4317.14-Å) and λ(4319.63-Å) lines with an O_2^+ beam, we obtained a mean lifetime of 8.5 ± 0.6 nsec for the $3p\,^4P^0$ levels. Using a much weaker O^+ beam (≃0.18 μÅ), we obtained one decay curve as a check on the O_2^+ measurements. It yielded a value of 8.6 ± 0.5 nsec, in excellent agreement with those measurements. (In the latter measurement the uncertainty is that computed for the least-squares fit.)

In Table IV we compare our measurement with those of other investigators[5–7] and theory.[3]

C. $3p\,^2D^0 \rightarrow 3s\,^2P$

The λ(4414.91-Å) and λ(4416.98-Å) lines of this multiplet stand quite apart from any other O II lines. This is shown quite well in Fig. 10. The nearest O II lines listed in Refs. 3 and 4 are at 4406.02 and 4443.05 Å, but neither is observed. The nearest observed lines are weak He I lines at 4387.93 and 4437.55 Å, which present no problems whatsoever.

Using nine independent decay curves of the combined λ(4414.91-Å) and λ(4416.98-Å) lines, we got as the lifetime of $3p\,^2D^0$ levels, 11.6 ± 0.3 nsec.

TABLE IV. Lifetimes for the $2p^2(^3P)3p\,^4P^0$ multiplet of O II.

Investigators	λ (Å)	$J=\frac{5}{2}$	τ (nsec)	$J=\frac{3}{2}$
Clark and Head	4317.14 4319.63		8.5 ± 0.6	
Copeland[a]	4317.14			9.6
	4349.43	14.1		
Druetta, Poulizac, and Dufay[b]	4317.14			8.5
	4349.43	7.7		
Druetta and Poulizac[c]	4319.63	8.54		
	4349.43	7.7		
Theory[d]		9.8		9.2

[a]Reference 5.

[b]Reference 6.

[c]Reference 7. The wavelength assignments are based on their observed wavelengths and those tabulated in the National Bureau of Standards tables (Ref. 3).

[d]Reference 3.

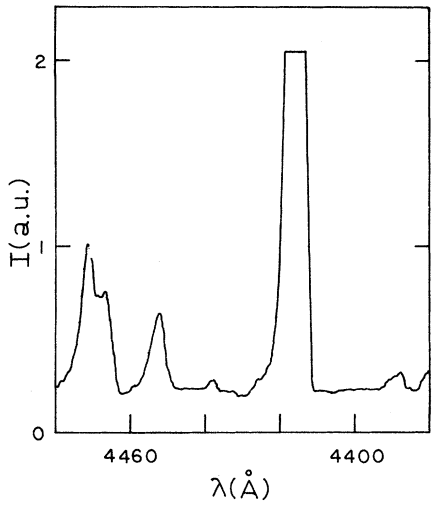

FIG. 10. Partial spectrum of an O_2^+ beam containing the principal members of the $3p\,^2D^0 \rightarrow 3s\,^2P$ and $3p'''\,^6P \rightarrow 3s'''\,^6S^0$ multiplets of O II. The line at 4471 Å is a He I line arising from the He target gas streaming through the exit aperture of the collision cell.

This value is compared with the results of others[3,6,7] in Table V.

D. $3p\,^2P^0 \rightarrow 3s\,^2P$

The transitions in this multiplet are shown in Fig. 11. The only lines which might blend with lines from this multiplet have wavelengths of 3967.44 and 3985.46 Å. Neither of these lines is in evidence in Fig. 11.

Using a spectral window of 6.4 Å (slit widths of 0.4 mm), we obtained three decay curves of the λ(3973.26-Å) line from which we extracted a mean lifetime of 9.2 ± 0.1 nsec for the $3p\,^2P^0_{3/2}$ levels. The value is compared with the results of other investigators[3,6,8] in Table VI.

E. $3p'\,^2F^0 \rightarrow 3s'\,^2D$

The principal lines in this transition are shown in Fig. 12 in relation to the lines of the $3p\,^4D^0$ → $3s\,^4P$ multiplet. No other lines listed by Refs. 3 and 4 are found to be present to blend with these lines at 4590.97, 4596.0, and 4596.17 Å. The monochromator slit widths were, therefore, usually set at 1.0 mm.

Nine decay curves were taken using an O_2^+ beam. The average of the measurements gave 12.1 ± 0.3 nsec for the lifetime of the $3p'\,^2F^0$ levels. One decay curve was taken using an O^+ beam and a spectral window of 6.4 Å as a check. It gave a value of 12.00 ± 0.45 nsec, again in excellent agreement with the O_2^+ results.

Our result is compared with the results of others[3,5-9] in Table VII.

F. $3p'\,^2D^0 \rightarrow 3s'\,^2D$

The lines in this multiplet are included in Fig. 9. Because of the high resolution required, with the resulting low intensities, only three decay curves were obtained, all on the combined λ(4351.27-Å) and λ(4351.5-Å) lines (both $J = \frac{5}{2}$). The mean of these three measurements was 9.2 ± 0.4 nsec. This result is compared with those of other investigators[3,8] in Table VIII.

G. Other Multiplets

Measurements on five other multiplets have been made. These results are shown in Table IX. Unfortunately, however, these results are suspect because of possible streaming errors and should be taken only as upper limits on the lifetimes of the associated levels.

The $3d'\,^2G \rightarrow 3p'\,^2F^0$ transitions were the only ones listed in Table IX with sufficient intensity and spectral separation to enable us to get a decay curve using an O^+ beam. It gave a lifetime of

TABLE V. Lifetimes of the $2p^2(^3P)3p\,^2D^0$ multiplet of O II.

Investigators	λ (Å)	τ (nsec)
Clark and Head	{4414.91 / 4416.98}	11.6 ± 0.3
Druetta *et al.*[a]	{4414.91 / 4416.98}	11
Druetta and Poulizac[b]	4416	11.85
Theory[c]		8.7

[a]Reference 6.
[b]Reference 7.
[c]Reference 3.

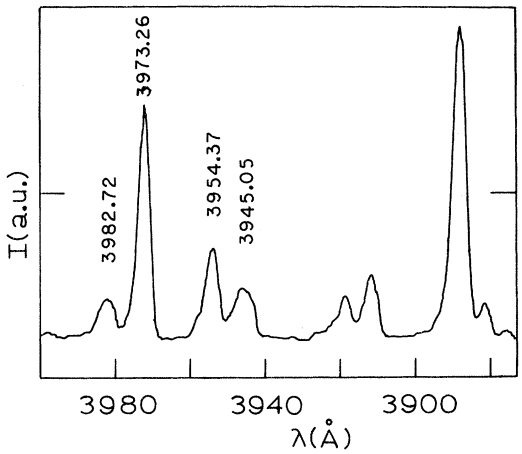

FIG. 11. Partial spectrum of an O_2^+ beam between approximately 3875 and 4000 Å. The lines for which the wavelengths are given are members of the $3p\,^2P^0 \rightarrow 3s\,^2P$ multiplet of O II.

TABLE VI. Lifetime of the $2p^2(^3P)3p\ ^2P^0$ multiplet of O II.

Investigators	λ (Å)	τ (nsec)
Clark and Head	3973.26	9.2 ± 0.1
Druetta *et al.*[a]	3973.26	7.1
Kernahen *et al.*[b]	3973.26	6.0 ± 0.5
Theory[c]		6.7

[a]Reference 6.
[b]Reference 8.
[c]Reference 3.

TABLE VIII. Lifetime of the $2p^2(^1D)3p'\ ^2D^0$ multiplet of O II.

Investigators	λ (Å)	τ (nsec)
Clark and Head	{4351.27 / 4351.5}	9.2 ± 0.4
Kernahan *et al.*[a]	2445.55	3.7 ± 0.3
Theory[b]		≤ 9.6

[a]Reference 8.
[b]Reference 3. The tables are incomplete for this level.

5.3 ± 0.7 nsec. Although O_2^+ and O^+ values can be considered to be in agreement, within the indicated errors, the O^+ result is sufficiently short to lead us to not have much faith in any of the measurements in Table IX. Another thing which makes them suspect is that they are all approximately the same, namely 6 nsec. The theoretical values, on the other hand, range from 3.8 to 7.1 nsec. Of course, the tables in Ref. 3 from which they were calculated may be incomplete.

IV. DISCUSSION OF ERRORS

Errors in our type of measurement may arise from blending with unwanted spectral lines, cascading from higher levels, population of the excited levels by collisions with the target gas which streams through the exit aperture, uncertainties in the speed of the beam ions, and uncertainties in the distance measurements. Let us consider these one at a time.

Nowhere in the region of the spectrum of interest did we find reproducible evidence of O I or O III lines. If any molecular bands were present, they were buried in the background noise. We do not believe that any significant errors occurred because of blending.

The problem of cascading, however, cannot be dismissed so easily. Figure 5 shows, for example, that electrons in the $4f'\ ^2H^0_J$ levels cascade into the $3d'\ ^2G_J$ levels. These levels, in turn, cascade into the $3p'\ ^2F^0_J$ levels. Several other levels also cascade into these latter levels; however, none of their associated transitions show up on our scans. Only the $3d'\ ^2G \rightarrow 3p'\ ^2F^0$ transitions appear with sufficient intensity to contribute significantly to the population of the $3p'\ ^2F^0$ levels; and, likewise, only the $4f'\ ^2H^0 \rightarrow 3d'\ ^2G$ transitions appear with sufficient intensity to contribute appreciably to the $3d'\ ^2G$ levels.

The experimentally determined lifetime of the $3d'\ ^2G$ levels is 6.1 ± 0.5 nsec, a value much shorter than the measured 12.1 ± 0.3 nsec for the lifetime of the $3p'\ ^2F^0$ levels. In such a situation, the coefficient B'_j of the cascade term in Eq. (6) should be negative, and the initial part (that is, that part at small x) of the decay curve should fall off less rapidly than the main part of the curve. There is indeed some slight indication of an initial buildup in the $3p'\ ^2F^0 \rightarrow 3s'\ ^2D$ decay curves, but not to the extent shown in the curves in Figs. 4 and 8.

The decay curves in Figs. 4 and 8 are from $3p\ ^4D^0 \rightarrow 3s\ ^4P$ transitions. The $3p\ ^4D^0$ levels in this case should be heavily fed by cascade from the

TABLE VII. Lifetime of the $2p^2(^1D)3p'\ ^2F^0$ multiplet of O II.

Investigators	λ (Å)	τ (nsec)
Clark and Head	{4590.97 / 4596.0 / 4596.17}	12.1 ± 0.3
Copeland[a]	4590.97	10.5
Druetta *et al.*[b]	{4590.97 / 4596.0 / 4596.17}	14 14
Druetta and Poulizac[c]	4593	12.8
Pinnington and Lin[d]	{4590.97 / 4596.0 / 4596.17}	8.7 ± 0.3
Kernahan *et al.*[e]	4592	10 ± 1
Theory[f]		9.0

[a]Reference 5.
[b]Reference 6.
[c]Reference 7.
[d]Reference 9.
[e]Reference 8.
[f]Reference 3.

TABLE IX. Upper limits to the lifetimes of some short-lived O II levels.

Level	λ (Å)	τ (nsec)	Theory[a] τ (nsec)	Other results τ (nsec)
$3p\ ^4S^0_{3/2}$	3749.49	≤6.4 ± 0.8	5.6	5.8,[b] 4.8[c]
$3d\ ^4F_{9/2,7/2,5/2,3/2}$	4075	≤5.8 ± 0.5	5.1	5.6,[b] 5.29[d]
$3p'\ ^2P^0_{3/2}$	3911.96	≤6.0 ± 0.1	7.1	4.9[b]
$3d'\ ^2G_{9/2,7/2}$	4188	≤6.1 ± 0.5	4.0	9.5,[b] 6.1,[b] 5.1[d]
$4f'\ ^2H^0_{11/2,9/2}$	4254	≤5.9 ± 0.5	3.8	5.5,[b] 4.35,[d] 6.9[e]

[a]Reference 3.
[b]Reference 6.
[c]Reference 8.
[d]Reference 7.
[e]Reference 9.

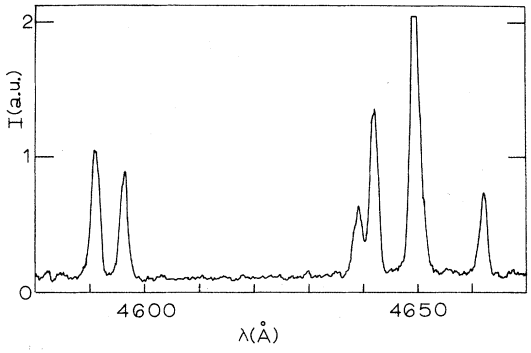

FIG. 12. Partial spectrum of an O_2^+ beam showing both the $3p\,^4D^0 \rightarrow 3s\,^4P$ multiplet (centered about 4650 Å) and the $3p'\,^2F^0 \rightarrow 3s'\,^2D$ multiplet (lines at 4596 and 4591 Å).

$3d\,^4F$ levels (judging from the intensity of the $3d\,^4F \rightarrow 3p\,^4D^0$ transitions centered around 4075 Å). (See Fig. 13 for the relative strength of these transitions as compared to that of the $3p\,^4D^0 \rightarrow 3s\,^4P$ transitions centered about 4649 Å.) The shapes of both Figs. 4 and 8, each taken on different lines, bear this out. Both have negative decay components with lifetimes in the 5–6-nsec range. These components are approximately one-quarter as large as the principal components initially, but they rapidly die out. Not removing them in the fits to the curves, by adding an extra exponential, could lead to an error of approximately 10% in the measured lifetimes, if all the points in the measured decay curves were used. Deletion of the first few points in each curve would reduce that error to less than 5%.

The decay curves for the $3p'\,^2F^0$ levels and the $3p\,^4D^0$ levels are the only ones, with one notable exception, which exhibit the buildup phenomenon mentioned above. It is not present, for example, in the $3p\,^2D^0$ levels which have a measured lifetime almost identical with that of the $3p'\,^2F^0$ levels. This leads us to the rather firm belief that the negative decay components seen in the $3p'\,^2F^0 \rightarrow 3s'\,^2D$ and $3p\,^4D^0 \rightarrow 3s\,^4P$ multiplets arise from cascade, rather than populating of the levels by gas streaming through the exit aperture of the collision chamber.

Intermediate-lived cascade components were observed in all but the $3p\,^4D^0$, $3p\,^2P^0$, $3p'\,^2D^0$, and $3p'\,^2P^0$ decay curves. The largest such contribution occurred in the $3d\,^4F$ and $3d'\,^2G$ curves, where cascading from intermediate-lived (approximately 25 nsec) levels accounted for roughly 40% of the total signal. For the $3p\,^2D^0$ and $3p'\,^2F^0$ levels, cascade contributed about 3 and 10%, respectively. For the rest of the levels affected by intermediate-lived cascade a typical figure was 25%.

There was a strong correlation between poor reproducibility of the lifetime results and the existence of cascade in the decay curves. Results not manifestly affected by cascade were reproducible to within 2–4%; on the other hand, when cascade was definitely present, the reproducibility was around 5–10%. We, therefore, feel that the spread in our reported results gives a good indication of the error introduced by cascading.

Although we cannot offer conclusive proof that gas-streaming errors are negligible, we can at least offer some self-consistent evidence that they are not important for the results in Tables II and IV–VII.

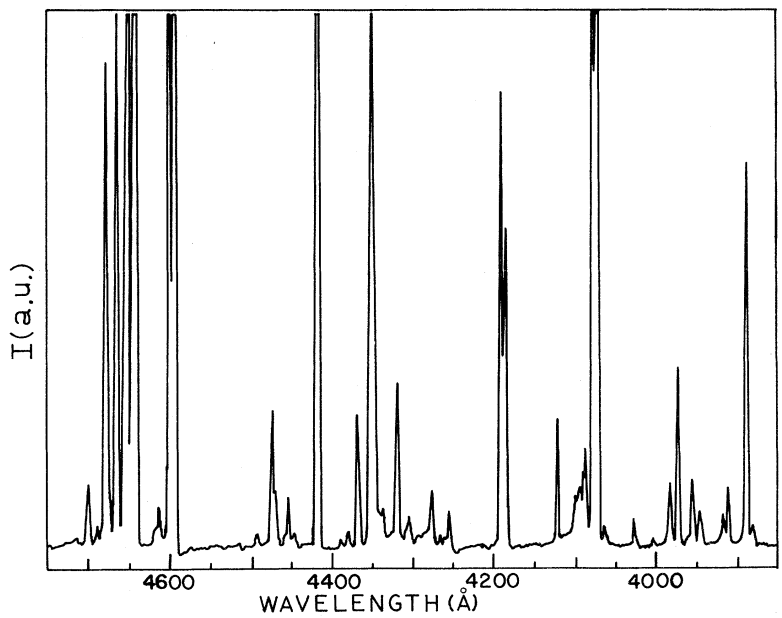

FIG. 13. More complete, but less detailed, spectrum of an O_2^+ beam from 3850 to 4750 Å. All lines observed are O II, except for He I lines at 3889 and 4471 Å.

As we indicated in Sec. II, the intensity of the He lines from the target gas streaming through the exit aperture of the collision chamber appears to drop off approximately as the sum of two exponentials. Better fits on the λ(5876-Å) He I line, however, involve sums of two exponentials and a constant, or sums of three exponentials. For example, the χ^2 integral for one such fit was 0.535. Since our χ^2 test was not entirely reliable, for reasons given earlier, visual inspection confirmed that the fit was indeed a good one, well within the error bars. The fast-decay constant and intermediate-decay constant were 11.1 and 3.3 cm^{-1}, respectively. These values are typical of those from several other independent curves.

The best fits to the He I λ(3889-Å) curves usually involved only sums of two exponentials. In only a few curves were we able to find an intermediate component similar to that in the λ(5876-Å) curves. Perhaps significantly, one of these was taken with 0.25-mm slit widths instead of the 0.4-mm widths usually needed for adequate intensity. The experimental curve is that shown in Fig. 2.

The main purpose in pointing out that such fits could be made is to show that the pressure outside the exit aperture might have dropped off more rapidly than indicated in Figs. 1 and 2. Indeed, if the fits mentioned above were valid, the pressure dropped off initially with a decay length of approximately 1 mm.

Other evidence to support this conclusion is the fact that an initial buildup (from a negative-decay component) was present in only a small fraction of the total number of decay curves measured. With the exception of one curve, observed buildup could be attributed, as shown in Sec. III, to cascading from short-lived levels. The lone exception occurred in a particularly good curve for the λ(4075.87-Å) line of the $3d\,^4F \rightarrow 3p\,^4D^0$ multiplet taken with 0.2-mm slit widths (see Fig. 6). It contained a small negative component with a decay length of about 1 mm.

This leaves the question of the origin and significance of the intermediate-decay component (if it really exists) in the He I curves mentioned above. We believe, as we indicated earlier in this paper, that it arose from a small velocity component imparted to the He atoms during collisions with the beam ions; otherwise, there should have been a significant negative component with a decay length around 3 mm in every decay curve. It should also have led to disagreement between the O_2^+ and O^+ results at decay constants of the principal components of around 3 cm^{-1} (corresponding to lifetimes of approximately 8.5 nsec). We have already pointed out that neither of these situations was encountered.

The fast-decay component, if actually present, would be of little consequence to our results, because omitting the first few mm of the decay curve would effectively eliminate it. The long-lived decay component, arising from the slowly decaying pressure component, presented no problem, because the computer program immediately converged to a fit on it. Errors in such fits contributed a small amount to the statistical uncertainty in the reported results.

The only uncertainty in the speed of the ions arose from the uncertainty in determining the accelerating voltage. The typical uncertainty in the voltage was 1 kV out of 25 kV. This led to an uncertainty of about 2% in the speed of the ions.

A vernier scale was used to measure the distance of translation of the monochromator downstream. It could be read to 0.05 mm, whereas our decay curves extended over several cm. The error in distance was, therefore, negligible compared to other errors.

Although we have devoted a considerable portion of this paper to the problem of gas streaming in the pressure transition region near the exit aperture of the collision cell, our study of streaming effects has clearly not been an exhaustive one. There are many interesting problems which remain to be investigated with respect to this matter, but they are not crucial to this study and will be investigated in a later study. Insofar as the present O II work is concerned, we are confident that the transition region is sufficiently sharp that it causes no real problem for lifetimes greater than 8.5 nsec. The approximately constant residual gas pressure that existed throughout the observation region caused no difficulty whatsoever. That it introduces no appreciable systematic error has been adequately demonstrated by the good agreement of our results from earlier studies with those of other investigators using highly different techniques. In particular, we call attention to the result of an N_2^+ study[10] performed in our laboratory. Our measured lifetime for the $B^2\Sigma_u^+ (v'=0)$ level of N_2^+ was 58.6 ± 5 nsec. This is sufficiently long to reveal any errors caused by the residual target gas in the observation region. Our experimental lifetime for this level, however, is in excellent agreement with the following recent measurements: 59.2 ± 6.0 nsec by Hesser[11] (phase-shift method); 59.2 ± 4 nsec by Johnson and Fowler[12] (pulsed-electron excitation with delayed-coincidence detection); 61.3 ± 1.6 nsec by Gray, Morack, and Roberts[13] (pulsed-electron excitation with delayed-coincidence detection); and 58 ± 5 nsec by Dotchin and Chupp[14] (pulsed-proton-beam excitation with delayed-coincidence detection). It is also in agreement with the lifetime of 59 nsec obtained by Johnson and Fowler[12] from a reanalysis of some older work by Fink and Welge.[15]

The close agreement of our work with Hesser's phase-shift work continues to much shorter lifetimes. The Ne II values[2] measured in our laboratory, for example, are in virtually perfect agreement with Hesser's Ne II lifetimes.[16] Our Ne II study is in most respects comparable to the present O II study; thus, the good agreement of our Ne II results with the results from the very different phase-shift technique should support the accuracy claimed for our O II results.

It seems appropriate here to point out that the gas-streaming problem causes occasional controversy; for example, see the discussion following a paper by Moak *et al.*[17] The offending property is the lack of a sharp excitation cutoff point; i.e., a well-defined $x = 0$ position. The existence of such a point is definitely *not* required. One needs only to have a *change* in the excitation conditions and to be able to identify and extract the resulting proper decay component in order to obtain the radiative lifetime. We think that we have presented adequate evidence that this can be done, as long as the exponential decay of the level of interest does not coincide with an exponential decay in the pressure. We mean by this, of course, that the spatial decay lengths, as defined and used herein, for the two decay processes must not be equal.

ACKNOWLEDGMENTS

Several persons have contributed to the successful completion of this work. The authors hereby acknowledge those contributions and thank S. A. Chin-Bing, C. W. Schuler, M. Iovine, E. A. Branley, J. H. Rees, P. F. Carroll, N. Weaver, T. Lawrence, L. Maleki, D. King and M. E. Head.

†Based in part on the M.S. thesis of J. H. Clark.

*Present address: Department of Computer Science, University of Utah, Salt Lake City, Utah 84112.

[1]S. A. Chin-Bing, C. E. Head, and A. E. Green, Jr., Am. J. Phys. 38, 352 (1970).

[2]C. E. Head and M. E. M. Head, Phys. Rev. A 2, 2244 (1970). In the course of publication some parentheses in this paper were deleted, resulting in an error in the reported fast-decay constant on p. 2248. That value should read $(3\ \text{mm})^{-1}$; thus, the decay constant is 3.3 cm^{-1}, not 3 mm^{-1}.

[3]W. L. Wiese, M. W. Smith, and B. M. Glennon, *Atomic Transition Probabilities, H-Ne* (U. S. GPO, Washington, D. C., 1966).

[4]A. N. Zaidel' *et al.*, *Tables of Spectral Lines* (Plenum, New York, 1970), pp. 582–583.

[5]G. E. Copeland, J. Chem. Phys. 54, 3482 (1971).

[6]M. Druetta, M. C. Poulizac, and M. Dufay, J. Opt. Soc. Am. 61, 515 (1971).

[7]M. Druetta and M. C. Poulizac, Phys. Letters 29A, 651 (1969).

[8]J. A. Kernahan, C. C. Lin, and E. H. Pinnington, J. Opt. Soc. Am. 60, 986 (1970).

[9]E. H. Pinnington and C. C. Lin, J. Opt. Soc. Am. 59, 780 (1969).

[10]C. E. Head, Phys. Letters 34A, 92 (1971).

[11]J. E. Hesser, J. Chem. Phys. 48, 2518 (1968).

[12]A. W. Johnson and R. G. Fowler, J. Chem. Phys. 53, 65 (1970).

[13]D. Gray, J. L. Morack, and T. D. Roberts, Phys. Letters 37A, 25 (1971).

[14]L. W. Dotchin and E. L. Chupp, Bull. Am. Phys. Soc. 17, 574 (1972).

[15]Von E. Fink and K. W. Welge, Z. Naturforsch. 19a, 1193 (1964).

[16]J. E. Hesser, Phys. Rev. 174, 68 (1968).

[17]C. D. Moak, L. B. Bridwell, H. O. Lutz, S. Datz, and L. C. Northcliffe, in *Beam-Foil Spectroscopy*, edited by Stanley Bashkin (Gordon and Breach, New York, 1968), Vol. I, pp. 157–173.

PHYSICAL REVIEW A VOLUME 6, NUMBER 5 NOVEMBER 1972

Stability of Self-Consistent Symmetries in Atomic Theory: The Cases of Ne, F^-, and O^{--} †*

Roger F. Prat

Laboratoire de Photophysique Moléculaire,‡ Faculté des Sciences, 91-Orsay, France

(Received 5 March 1971; revised manuscript received 28 January 1972)

It is found that a nonspherical Hartree-Fock potential may occur even for atomic systems generally thought of as having a complete shell structure in their ground state. Some conditions, under which a perturbation treatment of correlation effects starting from deformed Hartree-Fock states may be performed, are discussed.

This paper aims at contributing to the discussion of the symmetry properties of atomic Hartree-Fock wave functions.[1,2] Although the result on the O^{--} ion may be of direct interest for the study of crystalline oxides,[1,3] the main purpose of this paper rather will be to show an example which is suggested by Kaplan's and Kleiner's[1] conclusion that the spherical symmetry of the self-consistent field may, or may not, depending on the atomic system, be a variational result even in a complete shell configuration.

This paper will be restricted to a singlet one-